

## MODEL OF STEERED TYRED WHEEL, THREE-DIMENSIONAL PROBLEM

ZBIGNIEW LOZIA

*Faculty of Transport, Warsaw University of Technology*  
*e-mail: lozia@alfa1.it.pw.edu.pl*

The paper presents a tyred wheel model. It describes an interaction between tyre and even as well as uneven road surface, in steady state or transient state. The influence of kingpin axis positioning as well as elastic properties of tyre and steering system is taken into account. The model results from a compromise between the following requirements: accuracy of phenomenon description, limitations of formal clearness, length of the computer program code, calculation time and feasibility of experimental verification of car movement simulation model. This tyred wheel model has been used effectively in simulation of biaxial vehicles movement and dynamics.

*Key words:* vehicle motion simulation, tyre model

### 1. Introduction

A model of tyred wheel is one of the main elements of simulation model of car's movement. It determines the qualitative and quantitative correctness of description of forces and moments generated within a zone of contact of the wheels with the road. Correct representation of the influence of three-dimensional positioning of the kingpin axis around which the steered wheel turns and to which elastic properties of the steering system and aligning moment of the wheels are reduced to also has significant importance in modelling.

Below, some works are listed, in which the reduction of forces existing in the contact of the wheel and road to the system fixed to axis of the kingpin which in effect gave a possibility of defining aligning moments of the steered wheels is presented. The simple calculation methods were employed, using only

geometric relations (cf Cronin, 1981; Lugner, 1981; Mitschke, 1977; Nordmark, 1984; Parraga, 1971; Studziński, 1980) or complex algorithms based on vector calculus (cf Berkefeld, 1983; Hiller and Woermie, 1985; Knapczyk and Kuranowski, 1986, 1987; Mitschke, 1977). Wicher (1995) considers the forces of inertia, which appear during transient states of the steering system movements, whereas other works include description of distortions of the elastic rubber-and-steel elements (silentblocks) (cf Berkefeld, 1983; Knapczyk and Kuranowski, 1986, 1987) as well as description of multi-arm suspension systems (cf Hiller and Woermie, 1985).

Much attention has been devoted to the interaction of vehicle with road through a such flexible element as the tyred wheel. Three-dimensional, elastic properties of the pneumatic tyre were described in terms of a matrix transforming the coupled linear and angular distortions of the tyre to the forces and moments (cf Bielecki, 1976; Bielecki and Maryniak, 1978). A model of string or ring with the elastic support (cf Pacejka, 1981; Zegelaar et al., 1994) were used or complex FEM models were applied (cf Böhm, 1979, 1989, 1993; Springer et al., 1989; Watanabe, 1984; Willumeit and Böhm, 1995) reflecting elastic properties in the range of frequencies up to 1000 Hz (cf Böhm, 1979, 1989, 1993) both in stationary and transient states (cf Springer et al., 1989; Willumeit and Böhm, 1995).

Bernard et al. (1981), Captain et al. (1979), Khachaturov et al. (1976), Davis (1975), Dunn and Olatunbosun (1989), Jackowski and Prochowski (1994), Lozia (1985), (1988), Lomako and Veremeev (1993) concentrated mainly on correct simulation of the elastic-damping forces (or elastic only) generation acting in radial direction in the plane of wheel. These models enable one to describe the forces resulting from the contact of the wheel with an uneven, rigid road surface with the lengths of irregularities comparable with those of the footprint. Lozia (1988) gave the description of radial and tangential (circumferential) forces for the above mentioned irregularities.

Largest number of publications has been devoted to description of forces and moments in the contact zone between wheel and road. Jędrzejczak (1980), Lozia (1985), Maryniak (1976), Mitschke (1977) presented the review of earlier efforts. In addition to description of the results of experimental studies of tyres (cf Baciński, 1969; Bakker et al., 1987; Bobrowski and Prochowski, 1989; Clark, 1981; Pacejka and Bakker, 1993; Sakai, 1981, 1982; Takahashi and Pacejka, 1988), numerous theoretical works were made, aimed at formulation of analytical description of tangential longitudinal (circumferential) force and the lateral one as well as the aligning moment of tyre (cf Dugoff et al., 1970; Fortunkov, 1980; Gim and Nikraves, 1990, 1991; Maalej et al., 1989;

Mastinu and Fainello, 1992; Pacejka, 1972; Pacejka and Sharp, 1991; Palkovics and El-Gindy, 1993; Palkovics et al., 1994; Sakai, 1981, 1982; Sharp and El-Nashar, 1986, 1993). Currently most frequently used for this purpose are the semi-empirical models (cf Bakker et al., 1987; Dugoff et al., 1970; Fancher and Bareket, 1993; Maalej et al., 1989; Pacejka and Bakker, 1993) which consist of approximations of experimental results. Despite a very close relation with a specific object and road surface, they are being used more and more frequently and so become a kind of standard in the simulation studies (HSRI-UMTRI model – see Dugoff et al., 1970, Fancher and Bareket, 1993; and "Magic Formula" – see Bakker et al., 1987, Pacejka and Bakker, 1993).

The most recent generation of models describing forces and moments in the tyre footprint are "Neuro-Tyre"-type models (cf Palkovics and El-Gindy, 1993; Palkovics et al., 1994), an application of the neural network method.

The models of transient states of interaction between tyre and road (cf Apetaur, 1993; Goraj, 1982; Mitschke, 1977; Palkovics et al., 1994; Takahashi and Pacejka, 1988; Willumeit and Böhm, 1995) are gaining more and more importance. Their applications allow for simulation of dynamic phenomena in the case of uneven road surfaces as well as better description of the "shimmy" – type phenomenon.

Below, the idea of a model of steered tyred wheel which enables description of many of the above mentioned phenomena is presented. It results from a compromise between the following requirements: accuracy of the phenomenon description, limitations of formal complexity, length of the computer code, calculation time and feasibility of experimental verification of the car movement simulation model. This tyred wheel model has been used effectively in simulation of biaxial vehicles movement (cf Lozia, 1993; Lozia and Stegienka, 1996).

## 2. Primary assumptions

The model of tyred wheel is an element of car movement simulation model (Fig.1). It should enable us to describe tyre footprint forces and elastic-damping properties of the front and rear wheels (steered and non-steered) and make allowance for geometric and kinematic properties of the steering system as well as elastic properties of the steering knuckle guidance system. It has been assumed that the road surface is uneven and undeformable. The road profile may result from real road measurements or realization of the random

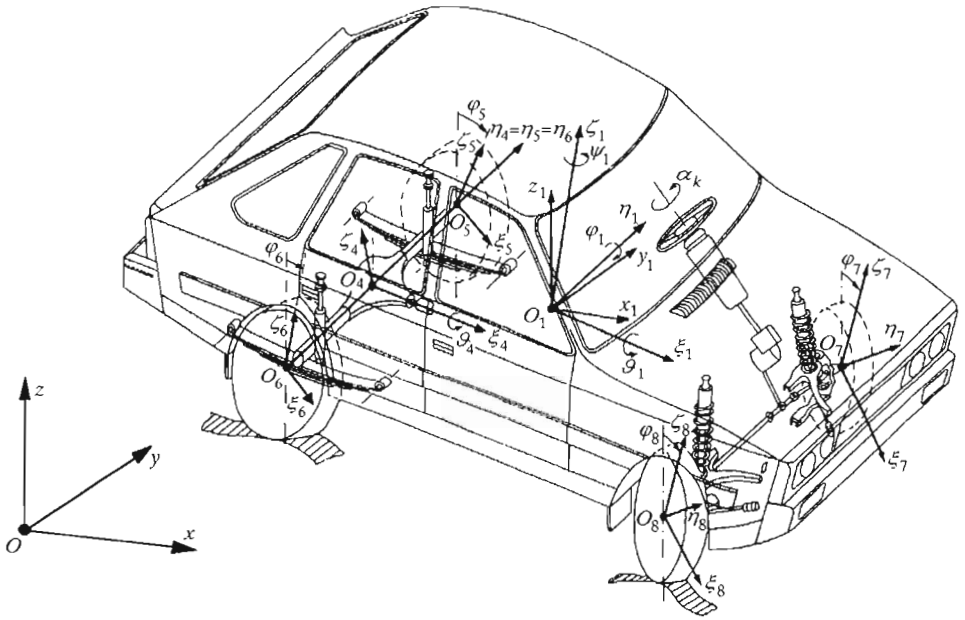


Fig. 1. Structure of the biaxial car model with the coordinate systems adopted

process (according to ISO/TC 108/253 recommendations) described using the bicubic spline interpolation. In the region of contact geometrical properties of the road are represented by the plane  $\pi_8$  tangential to the three-dimensional road profile (Fig.2).

Since we examine the surface irregularities longer at least several times than the largest dimension of the contact zone. Shorter irregularities are being averaged within the footprint area. We analyze the case in which (Fig.2) the tyred wheel interacts with the road plane  $\pi_8$  and we know: camber angle  $\varphi_{c8}$  related to the normal vector of this surface, normal reaction  $\mathbf{N}_8$ , velocity of the wheel center, longitudinal (circumferential) slip and lateral slip angle. In such a case it is always possible to use one of the known, experimentally verified models of interaction between the tyred wheel and flat road surface. Among the geometric properties of suspension only those influencing strongly the properties of tyred wheel model have been described. The relations representing the model are demonstrated on the example of front, right-hand side wheel.

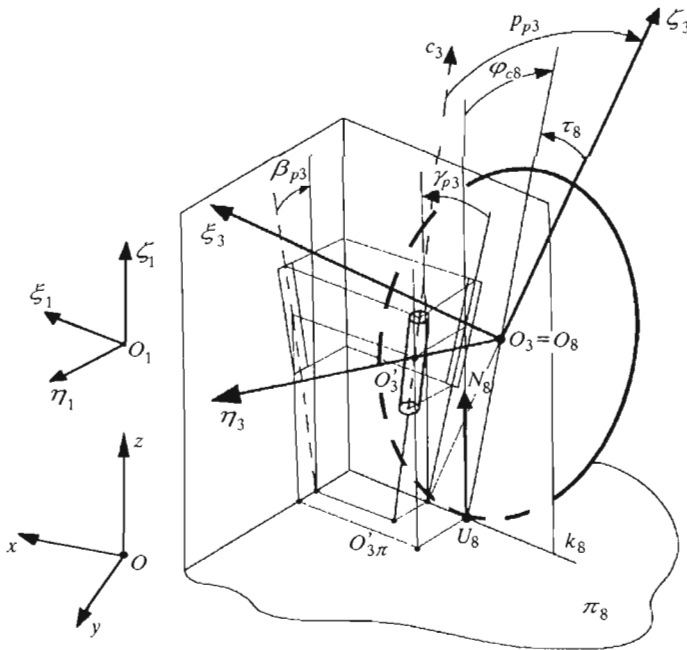


Fig. 2. Position of the kingpin axis  $O'_3O'_3\pi$  in the body-fixed system  $O_1\xi_1\eta_1$  (angles  $\beta_{p3}, \gamma_{p3}$ ) and of the tyred wheel relative to the plane  $\pi_8$  tangential to the road surface at point of contact  $U_8$  (angle  $\varphi_{c8}$ ). Here the plane  $\pi_8$  is horizontal ( $\varphi_{c8} = \varphi_{c3}$ ), and the steering angle of the wheel is equal to zero. Elastic deformations of the steering system have not been shown. Right-hand side, front wheel

### 3. Coordinate systems used for description of the vehicle movement

Vehicle motion is described in the inertial reference system  $Oxyz$  connected with the road (Fig.1). In the center of the vehicle's body mass  $O_1$  there has been attached a movable system  $O_1x_1y_1z_1$  with the axes parallel to respective axes of the inertial system. The system  $O_1\xi_1\eta_1\zeta_1$  is rigidly connected with the body. The angles:  $\psi_1$  (yaw),  $\varphi_1$  (pitch),  $\vartheta_1$  (roll) describe the body rotation about a fixed point  $O_1$ . In the middle of the rear axle  $O_4$  (dependent suspension) there has been attached the system  $O_4\xi_4\eta_4\zeta_4$  rigidly connected with the axle. Together with the wheels rotate the systems attached in the centers of the wheels. These are denoted by  $O\xi\eta\zeta$  with indices 7,8 and 5,6 defining location of the wheels in the vehicle. This model of the vehicle has 14 degrees of freedom (Fig.1:  $x_{O_1}, y_{O_1}, z_{O_1}, \psi_1, \varphi_1, \vartheta_1, \zeta_{1O_4}, \vartheta_4, \zeta_{1O'_2}, \zeta_{1O'_3},$

$\varphi_5, \varphi_6, \varphi_7, \varphi_8$ , where  $O'_2$  and  $O'_3$  are the points of intersection of kingpins with the axes of wheels rotation).

#### 4. Geometric properties of the suspension and geometric-elastic properties of steering column, steering gear and steering knuckle system

Three-dimensional location of the kingpin axis is described (Fig.2) in the body-fixed system  $O_1\xi_1\eta_1\zeta_1$  by angles: kingpin inclination  $\beta_{p3}$  and castor angle  $\gamma_{p3}$ . Apart from this the wheel plane is the angle of  $p_{p3}$  from the kingpin and angle of  $\varphi_{p3}$  from the vertical and  $\varphi_{c8}$  from the normal to the contact plane.

For the independent suspension the angles  $\beta_{p3}$  and  $\gamma_{p3}$  are functions of its deflection

$$\beta_{p3} = \beta_{p3}(\zeta_{1O'_3}) \quad \gamma_{p3} = \gamma_{p3}(\zeta_{1O'_3}) \quad (4.1)$$

For a dependent suspension these angles are also functions of deflection of the other wheel

$$\beta_{p3} = \beta_{p3}(\zeta_{1O'_3}, \zeta_{1O'_2}) \quad \gamma_{p3} = \gamma_{p3}(\zeta_{1O'_3}, \zeta_{1O'_2}) \quad (4.2)$$

Driver is acting upon the vehicle by changing the steering wheel angle  $\alpha_k$ . The arm of the steering gear is rotated by angle  $\alpha_w$  which is a function of the angle  $\alpha_k$ , steering gear ratio  $i_k$  and aligning moments  $R_{2c2}, R_{3c3}$  of the left and right road wheel

$$\alpha_w = \alpha_w(\alpha_k, i_k, R_{2c2}, R_{3c3}) \quad (4.3)$$

Therefore, there has been taken into account the flexibility of steering column and gear.

The steering angle of the wheel about the axis of the kingpin  $\alpha_{p3}$  is a function of  $\alpha_k$ , suspension deflections of both wheels  $\zeta_{1O'_3}$  and  $\zeta_{1O'_2}$ , wheel toe-in angle  $\alpha_{z3}$  and elastic deformation of the steering-linkage system which is a function of aligning moments  $R_{2c2}$  and  $R_{3c3}$

$$\alpha_{p3} = \alpha_{p3}(\alpha_k, \zeta_{1O'_3}, \zeta_{1O'_2}, \alpha_{z3}, R_{2c2}, R_{3c3}) \quad (4.4)$$

The functions which appear in Eqs (4.1) ÷ (4.4) are defined experimentally or result from the analysis of geometric and kinematic properties of suspension.

The wheel plane relative velocities (observed in the system  $O_1\xi_1\eta_1\zeta_1$ ) resulting from Eqs (4.1) ÷ (4.4) are neglected because they are many orders lower than those resulting from the considered degrees of freedom (Fig.1:  $x_{O_1}, y_{O_1}, z_{O_1}, \psi_1, \varphi_1, \vartheta_1, \zeta_{1O_4}, \vartheta_4, \zeta_{1O'_2}, \zeta_{1O'_3}, \varphi_5, \varphi_6, \varphi_7, \varphi_8$ ).

**5. Elastic properties of the steering knuckle guidance system**

In the majority of constructions the steering knuckle guidance system consists of: upper and lower A-arms with joints seated flexibly using rubber-and-steel elements (silentblocks), transverse link and McPherson strut with flexibly seated joints (McPherson suspension), leaf spring working as a guide, and rigid axle flexibly seated. The vector

$$w_{k3} = \text{col}[\gamma_3, \beta_3, \alpha_3] \tag{5.1}$$

defines the angular position of the steering knuckle in the body-fixed  $O_1\xi_1\eta_1\zeta_1$  system. Elastic deformations of the guidance system are taken into account since the elements of this vector are sums of the values resulting from geometric properties of the suspension and steering system (Eqs (4.1) ÷ (4.4)) as well as angular deformations of the steering knuckle guidance system caused by the resultant moment  $R_3$

$$w_{k3} = w_{p3} + D_3 R_3 \tag{5.2}$$

where  $D$  – matrix of angular flexibility of the steering knuckle guidance system and

$$w_{p3} = \text{col}[\gamma_{p3}, \beta_{p3}, \alpha_{p3}] \quad R_3 = \text{col}[R_{3a3}, R_{3b3}, R_{3c3}] \tag{5.3}$$

$R_3$  is the resultant moment of the system of forces acting upon the tyred wheel, reduced to the point  $O'_3$  and the components defined in the  $O'_3a_3b_3c_3$  system, where  $O'_3$  is the point of intersection of steering knuckle kingpin axis  $O'_3c_3$  and the axis of rotation of the wheel  $O'_3\eta_3$ , whereas  $O'_3a_3$  is parallel to the plane of wheel.

Because of high rigidity of the steering knuckle, changes in the angle  $p_{p3}$  caused by the system of forces acting on the wheel have been neglected.

**6. Elastic properties of the steering system**

Elasticity of the steering column and steering gear has been taken into

account in Eq (4.3), elasticity of the steering linkage – in Eq (4.4), and elasticity of the steering knuckle guidance system in Eq (5.2), respectively. Such a method of making allowance for the elastic properties of the steering system seems to be troublesome but nevertheless it allows us to apply the model described about in a simple way to defining flexible properties of steered and as well as non-steered wheels guidance system.

### 7. Model of elastic-damping properties of the tyred wheel

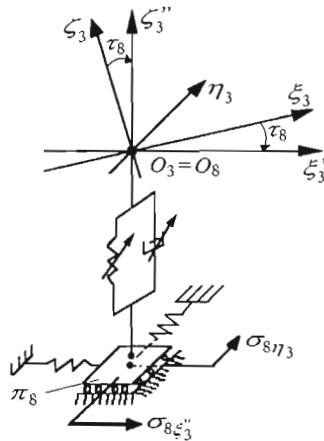


Fig. 3. Model of elastic-damping properties of tyre along the radial direction  $O_3\zeta_3''$  and elastic properties in the longitudinal  $\sigma_{8\xi_3''}$  and lateral  $\sigma_{8\eta_3}$  directions.  
Right-hand side, front wheel

Tyre elastic-damping properties in a radial direction and only elastic properties in longitudinal and lateral directions have been taken into consideration (Fig.3). Generally, the elastic-damping characteristics are non-linear and they are being approximated by polynomials. Adoption – for the radial properties – of the "point-contact tyre model" (cf Captain et al., 1979; Khachaturev et al., 1976; Lozia, 1985) results from the assumption that the area of contact with uneven road surface is a sector of the plane  $\pi_8$  tangential to the road at the center of footprint. Irregularities of the road are being averaged in this area (heights and inclinations in two perpendicular directions  $x$  and  $y$ ) which makes the applied model similar to the "fixed-footprint tyre model" (cf Captain et al., 1979; Khachaturev et al., 1976; Lozia, 1985). Such a procedure



is justified by the fact that irregularities of the road shorter than the length of footprint are the source of oscillation of pneumatic tyre forces with the frequencies higher by several orders than the vehicle model natural frequencies. They are not significant for the analysis of the vehicle's movement.

## 8. Model of tangential properties of the tyred wheel

In accordance with the assumptions adopted here, any model of tangential (shear) properties of the pneumatic tyre can be applied – which can generally be noted analytically in the following way (without the indices identifying the wheel)

$$\begin{aligned}\mu_w &= \frac{B_w}{N} = \mu_w(v, s_w, \delta, N, \varphi_c, \dot{s}_w, \dot{\delta}, \dot{N}, \dot{\varphi}_c) \\ \mu_p &= \frac{B_p}{N} = \mu_p(v, s_w, \delta, N, \varphi_c, \dot{s}_w, \dot{\delta}, \dot{N}, \dot{\varphi}_c) \\ R_n &= R_n(v, s_w, \delta, N, \varphi_c, \dot{s}_w, \dot{\delta}, \dot{N}, \dot{\varphi}_c)\end{aligned}\quad (8.1)$$

where

- $\mu_w$  – coefficient of longitudinal adhesion
- $\mu_p$  – coefficient of lateral adhesion
- $R_n$  – aligning moment in the direction normal to the area of contact, reduced to the center of footprint or the center of wheel
- $B_w$  – tangential longitudinal force, in the plane of footprint
- $B_p$  – tangential lateral force, in the plane of footprint
- $N$  – normal reaction of the road
- $v$  – projection of the center of wheel velocity on the plane of footprint
- $s_w$  – relative longitudinal (circumferential) slip
- $\delta$  – angle of lateral slip
- $\varphi_c$  – angle of wheel inclination relative to the normal to the plane of contact.

$\dot{s}_w, \dot{\delta}, \dot{N}, \dot{\varphi}_c$  – time derivatives of  $s_w, \delta, N, \varphi_c$ .

Taking into consideration the influence of  $\dot{s}_w, \dot{\delta}, \dot{N}, \dot{\varphi}_c$  on the magnitudes values of forces and moment acting in the footprint enables us to describe transient states during the tyred wheel movement.

9. Systems of coordinates used for transformation from the system  $O_1\xi_1\eta_1\zeta_1$  fixed to the vehicle body to the system  $O_8\xi_8\eta_8\zeta_8$  connected with wheel

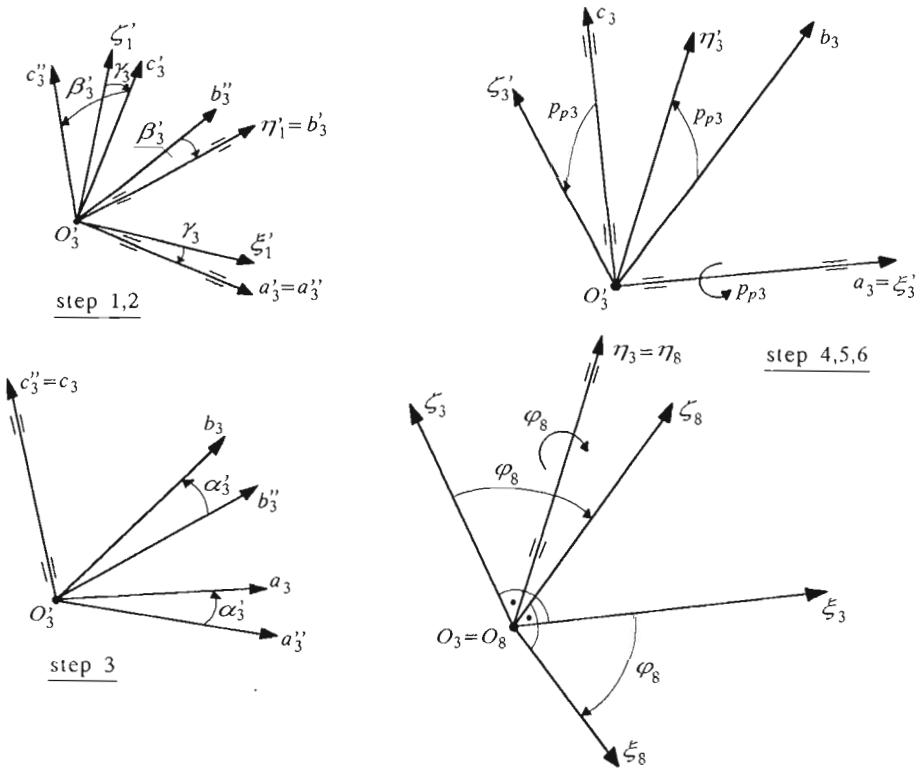


Fig. 4. Coordinate systems used for transformation from the body-fixed system  $O_1\xi_1\eta_1\zeta_1$  to the system  $O_8\xi_8\eta_8\zeta_8$  fixed to the right-hand side front road wheel

At the point  $O'_3$  of intersection of the kingpin axis with the wheel axis of rotation the system  $O'_3\xi'_1\eta'_1\zeta'_1$  has been attached (Fig.4), with the axes parallel to the axes of the system  $O_1\xi_1\eta_1\zeta_1$ , respectively. Rotation has been executed about axis  $O'_3\eta'_1$  by the castor angle  $\gamma_3$ .

Next, the resulting system  $O'_3a'_3b'_3c'_3$  has been rotated by the angle  $\beta'_3$  which is the projection of castor angle  $\beta_3$  onto the plane  $O'_3b'_3c'_3$

$$\beta'_3 = -\arcsin \frac{-\cos \gamma_3}{\sqrt{\cos^2 \gamma_3 + \cot^2 \beta_3}} \tag{9.1}$$

The system  $O'_3a''_3b''_3c''_3$  was obtained.  $O'_3c''_3$  is the axis of kingpin.

The third rotation is about axis  $O'_3c''_3$  by angle  $\alpha'_3$ . This creates the system  $O'_3a_3b_3c_3$ . The axis  $O'_3c_3$  coincides with the axis  $O'_3c''_3$  - it is the axis of kingpin. The angle  $\alpha'_3$  should ensure position of the axis  $O'_3a_3$  in the plane parallel to the wheel plane

$$\alpha'_3 = \alpha_3 + \arcsin \frac{1}{\sqrt{\left(\frac{\cos \beta'_3 \cos \varphi_{p3} + \sin \beta'_3 \cos \gamma_3 \sin \varphi_{p3}}{\sin \gamma_3 \sin \varphi_{p3}}\right)^2 + 1}} \tag{9.2}$$

The second element of this relation results from the necessity for compensation of the component of the wheel turn which is the consequence of earlier rotation by the angle  $\gamma_3$ .

The fourth turn takes place around axis  $O'_3a_3$  by the angle  $p_{p3}$ . The plane  $O'_3\xi'_3\zeta'_3$  of the system  $O'_3\xi'_3\eta'_3\zeta'_3$  created as a result of this turn is parallel to the plane of wheel.

Translation by the vector

$$s_3 = \text{col}[\xi'_{3O_3}, \eta'_{3O_3}, \zeta'_{3O_3}] \tag{9.3}$$

enables one to pass to the system  $O_3\xi_3\eta_3\zeta_3$  fixed at the center of wheel  $O_3 = O_8$ .

Rotation by  $\varphi_8$  (angle of rotation of the wheel) enables one to pass to the system  $O_8\xi_8\eta_8\zeta_8$  fixed to the wheel rim.

Knowing the coordinates of the center of mass of the body  $O_1$  in the inertial system  $Oxyz$ , knowing the transformation matrix of the body rotation about fixed point (angles  $\psi_1, \varphi_1, \vartheta_1$ ), as well as the matrix defining the above described transformations one can calculate the coordinates of any point of the wheel in the inertial system  $Oxyz$  and in system fixed to the vehicle body  $O_1\xi_1\eta_1\zeta_1$ .

### 10. Forces and moments appearing in the footprint

In order to calculate the forces transmitted by the tyred wheel we have to define the coordinates of the point of contact  $U_8$  and the coordinates of location and components of velocity of this point relative to the center of wheel  $O_3$ . This is the reason why calculations are made within the moving systems linked to the vehicle body. Additionally, because the irregularities of the road surface are defined in the inertial reference system  $Oxyz$ , the calculations also have to be made in that system. Fig.5 shows the resultant

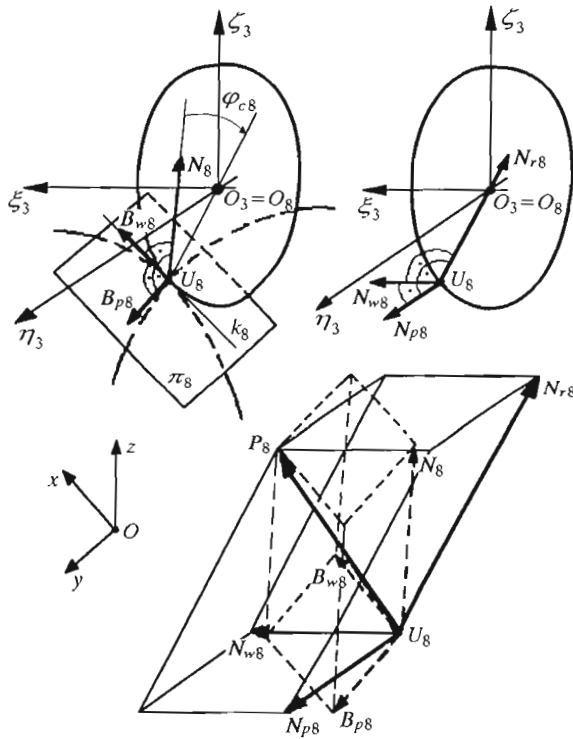


Fig. 5. Two equivalent force systems at the contact point  $U_8$  between the tyred wheel and road

vector of contact forces  $P_8$ . This is the resultant for the two systems of three mutually perpendicular vectors:

- System of three forces related to the road  $N_8, B_{w8}, B_{p8}$  (the reaction normal to the road profile and two tangential reactions located in the plane of contact  $\pi_8$ : the longitudinal one, at the same time located in the plane parallel to the plane of the wheel and lateral, perpendicular to  $k_8$ , the line of intersection of the road plane  $\pi_8$  and the plane of wheel); these forces are defined using the tyre tangential (shear) properties model Eqs (8.1).
- System of forces related to the wheel  $N_{r8}, N_{w8}, N_{p8}$  (the radial reaction and longitudinal reaction – perpendicular to the former – located in the plane parallel to the plane of wheel and the lateral reaction, perpendicular to the plane of wheel); these forces are defined using a model of elastic-damping properties of tyre.

The algorithm of calculations of modules and components of versors for these six forces is as follows.

Basing on the current values of coordinates of the body center of mass  $x_{O_1}, y_{O_1}, z_{O_1}$ , the angles defining body rotation about the fixed point  $O_1(\psi_1, \varphi_1, \vartheta_1)$ , the coordinate  $\zeta_{1O'_3}$  of relative movement of point  $O'_3$  as well as the angles  $\gamma_3, \beta_3, \alpha_3, p_{p3}$ , coordinates and velocities of the center of wheel  $O_3$  are defined in the inertial reference system  $Oxyz$ .

The point  $T_3$  (not shown in Fig.5) is taken as the first approximation of the wheel and road contact point  $U_8$ . This point is the intersection point of the road surface and a straight line, the edge of intersection of the wheel plane and a vertical plane, perpendicular to the wheel plane and crossing its center. In order to simplify and speed-up the calculations, we look for a point lying on this line at the distance equal to the length of dynamic radius approximated by the value from the previous step of simulation. Next, using similar approximation of magnitudes of forces  $N_{r8}$  and  $N_{p8}$  we calculate the longitudinal and lateral dislocations of the center of footprint  $\sigma_{8w}, \sigma_{8p}$  which are then transformed to the inertial reference system  $(\sigma_{8x}, \sigma_{8y}, \sigma_{8z})$

$$\sigma = \text{col}[\sigma_{8x}, \sigma_{8y}, \sigma_{8z}] \tag{10.1}$$

The coordinates of the point of contact  $U_8$  are being calculated as

$$x_{U8} = x_{T3} + \sigma_{8x} \qquad y_{U8} = y_{T3} + \sigma_{8y} \tag{10.2}$$

The height of profile  $z_{U8}$  and the angles of inclination of the plane of contact  $\pi_8$  in directions  $x$  and  $y$ :  $\varepsilon_{8x}, \varepsilon_{8y}$  are being calculated basing on description of the road profile in the following form

$$z_{U8} = z_U(x_{U8}, y_{U8}) \qquad \varepsilon_{8x} = \varepsilon_x(x_{U8}, y_{U8}) \qquad \varepsilon_{8y} = \varepsilon_y(x_{U8}, y_{U8}) \tag{10.3}$$

The length  $r_8$  of projection of the vector  $U_8O_8$  onto the wheel plane  $O_3\xi_3\zeta_3$  is being treated as dynamic radius of the pneumatic tyre. This projection enables us to define the versor  $n_{r8}$  of the radial force  $N_{r8}$  and the angle of rotation  $\tau_8$  of the system  $O_3\xi_3\eta_3\zeta_3$  about the axis  $O_3\eta_3$  in such a way that in thus created system  $O_3\xi_3''\eta_3''\zeta_3''$  (Fig.3) the axis  $O_3\zeta_3''$  has the direction of force  $N_{r8}$  and  $O_3\xi_3''\zeta_3''$  is the wheel plane. Knowing the projections of the center of wheel velocity onto the plane  $Oxy$  and the inclinations of road surface  $\varepsilon_{8x}, \varepsilon_{8y}$  we may calculate the velocity  $dz_{U8}/dt$  and the vertical component of relative velocity  $dU_8O_8/dt$ , and next (knowing components of versor  $n_{r8}$ ) the velocity of radial deflection  $dr_8/dt$  of the tyre. The module of radial force is a function defined in the course of experimental studies

$$N_{r8} = N_r \left( r_8, \sigma_{8w}, \sigma_{8p}, \frac{dr_8}{dt} \right) \tag{10.4}$$

The next step is to calculate the geometric and kinematic parameters of tangential interaction with the road:  $\varphi_{c8}, s_{w8}, s_{p8}, v_8$ . They are functions of generalized coordinates and parameters of the model. Using the tyre tangential (shear) properties model Eqs (8.1) we calculate the values of coefficients of adhesion  $\mu_{w8}, \mu_{p8}$  as well as the aligning moment  $R_{n8}$ . The module of road normal reaction  $N_8$  is being approximated here using the value from the previous step of simulation.

As we see in the above, for the six vectors shown in Fig.5 we know:

- module of radial force  $N_{r8}$
- versors of vectors  $N_{w8}, N_{p8}, N_{r8}$  (respective versors of the axes of system  $O_3\xi_3''\eta_3''\zeta_3''$ )
- versor of the force  $B_{w8}$  (versor of the edge  $k_8$ )
- versor of the force  $B_{p8}$  (vector product of normal vector versor of the contact plane  $\pi_8$  and versor of the edge  $k_8$ )
- versor of the force  $N_8$  (normal vector versor of the contact plane  $\pi_8$ ).

Unknown are the modules of vectors  $N_{w8}, N_{p8}, B_{w8}, B_{p8}, N_8$ . The last three bear the relations (also see Eqs (8.1))

$$B_{w8} = \mu_{w8}N_8 \qquad B_{p8} = \mu_{p8}N_8 \qquad (10.5)$$

The three remaining unknowns:  $N_{w8}, N_{p8}, N_8$  are being found as solutions of the system of equations created as the result of projecting the footprint forces onto axes of the system  $O_3\xi_3''\eta_3''\zeta_3''$

$$\begin{aligned} N_{w8} &= N_8 n_{8\xi_3''} + B_{w8} b_{w8\xi_3''} + B_{p8} b_{p8\xi_3''} \\ N_{p8} &= N_8 n_{8\eta_3''} + B_{p8} b_{p8\eta_3''} \\ N_{r8} &= N_8 n_{8\zeta_3''} + B_{w8} b_{w8\zeta_3''} + B_{p8} b_{p8\zeta_3''} \end{aligned} \qquad (10.6)$$

where  $n$  and  $b$  with indices 8,  $\xi_3'', \eta_3'', \zeta_3''$  represents the components of versors of respective vectors on the axes indicated by the indices.

Next, we calculate the values  $B_{w8}, B_{p8}$ , Eqs (10.5), the resultant vector of forces in the footprint  $P_8$  and the vector of aligning moment  $R_{n8}$  relative to the center of footprint.

The system of forces in the footprint is reduced to the center of wheel  $O_3$  and to the center of kingpin  $O'_3$ . In the latter case we take into consideration the fact that the component of the moment on the axis of rotation is not transferred as whole but only its part dependent on the value of angular deceleration and the moment of inertia of the wheel and the external torque (driving or breaking). So, we calculate the vector  $R_3$  (see Eq (5.3)).

## 11. Results of sample calculations

Applicability of the model shall be demonstrated on the example of tyre 165R13D124 and passenger car FSO Polonez. The geometric and elastic parameters of the tyre were adopted basing on static test stand studies. Geometrical parameters of the suspension and steering system were defined basing on the design drawings and laboratory measurements. Other values were estimated using specifications of tyres and car of similar class (cf Clark, 1981; Dugoff et al., 1970; Mitschke, 1977; Pacejka, 1972, 1981; Pacejka and Sharp, 1991; Sakai, 1981, 1982).

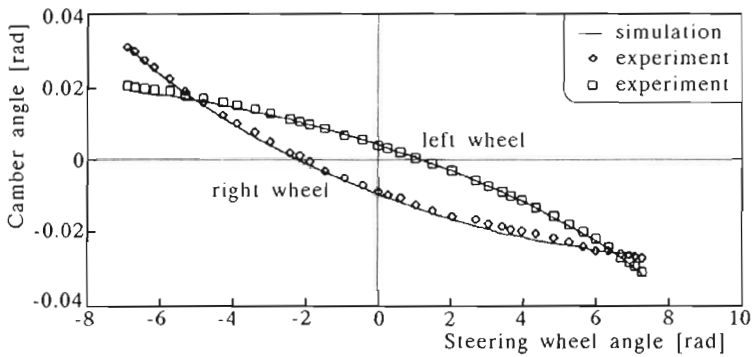


Fig. 6. Changes of the wheel camber angle  $\varphi_{p3}$  during turn which is the result of the rotation of steering wheel  $\alpha_k$ . The wheels transmit only the normal reaction of horizontal foundation. Passenger car FSO Polonez of the type

In order to verify geometric properties of the model the simulation has been performed of the phenomena occurring during turning of the wheels caused by a quasi-static application of the steering wheel angle. Wheels do not rotate, *instead they just sit on the so-called "turn-tables" which only transmit the normal reactions of the foundation.* Vertical position of the centers of wheels is calculated by iteration in such a way as to maintain with a given accuracy 1 N a constant magnitude of 3000 N of normal reaction. The parameters of the car model correspond the specimen of FSO Polonez under study. Fig.6 shows the results of simulation and the results of experimental tests of the wheel camber angle as a function of the angle of steering wheel rotation. A very good consistency, both qualitative and quantitative, between the simulation and experiment results is visible.

It was very hard to obtain the data describing tangential (shear) properties of the tyre. That is why a relatively simple in use the HSRI-UMTRI model

(cf Dugoff et al., 1970; Fancher and Bareket, 1993) has been applied. Specifications of similar tyres have been used (cf Clark, 1981; Dugoff et al., 1970; Mitschke, 1977; Pacejka, 1972, 1981; Pacejka and Sharp, 1991; Sakai, 1981, 1982).

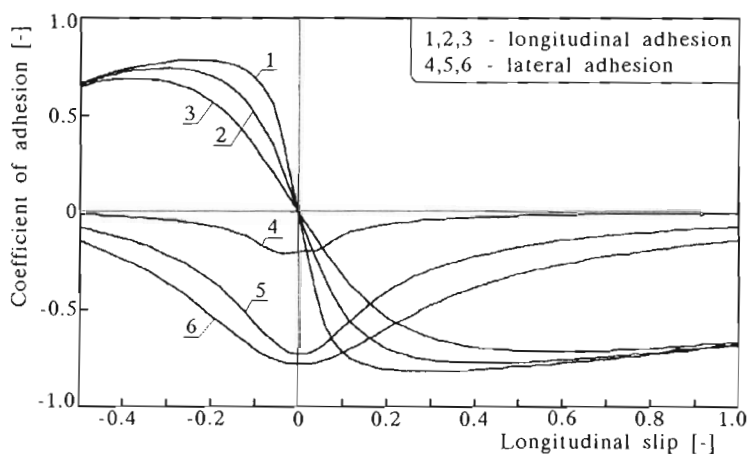


Fig. 7. Characteristics of the coefficients of longitudinal adhesion  $\mu_w$  (lines 1, 2, 3) and lateral adhesion  $\mu_p$  (lines 4, 5, 6) versus the relative longitudinal slip  $s_w$  (negative for drive, positive for braking) for constant values of the lateral slip angle  $\delta$  (zero for 1 and 4, 0.15 rad for 2 and 5, 0.3 rad for 3 and 6). Road surface: dry asphalt-concrete. Wheel cambar angle  $\varphi_{p3} = 0.1$  rad, normal reaction of road  $N_8 = 3000$  N. Velocity  $V = 10$  m/s. Results of simulation

Fig.7 shows the characteristics of coefficient of longitudinal and lateral adhesion on dry surface for constant values of lateral slip angle and the camber angle of 0.1 rad value.

The model of steered tyred wheel presented here has been put into use as an element of the simulation model of movement of biaxial passenger car FSO Polonez (cf Lozia, 1993; Lozia and Stegienka, 1996). Fig.8 and Fig.9 show sample results of simulation of a single lane change maneuver. The lane width was equal to 3.5 m. We used the time history of steering wheel angle, recorded during an experiment. Fig.8 presents the comparison between lateral accelerations of the vehicle: resulting from measurements (E) and simulation (S), respectively. Fig.9 shows the projection of trajectory of the center of mass of the vehicle body  $O_1$  onto the plane of road. Bold, solid lines define the boundaries of the first and second traffic lane. Both drawings prove correct functioning of the tyred wheel model. This applies to both qualitative as well as quantitative consistency.



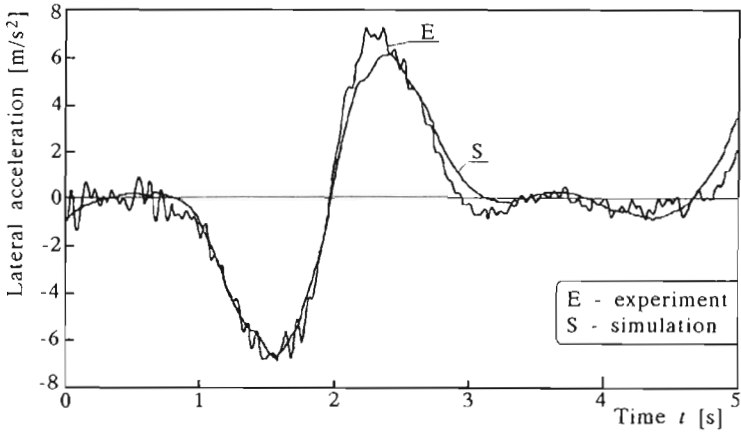


Fig. 8. Time histories of lateral acceleration during a single lane change maneuver. Experiment and simulation. Passenger car of the FSO Polonez type,  $V = 19.1$  m/s

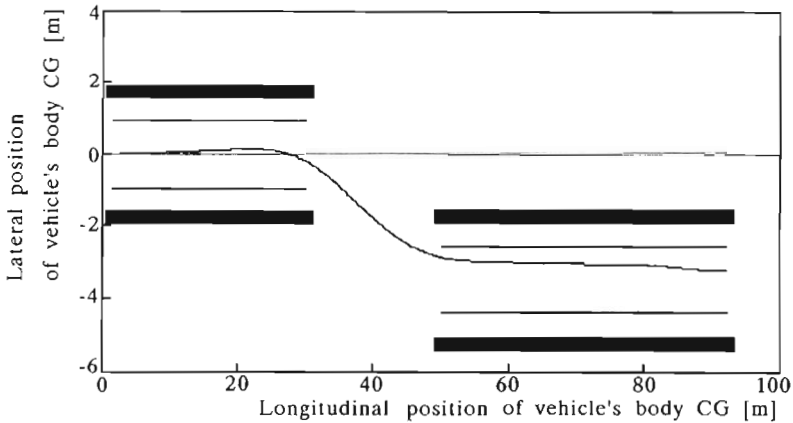


Fig. 9. Projection of trajectory of the center of body mass  $O_1$  of the FSO Polonez type car onto the plane of road during a single lane change maneuver,  $V = 19.1$  m/s. Results of simulation. Bold, solid lines define the boundaries of first and second traffic lanes

### Acknowledgments

The Author wishes to thank Mr. Wiktor Mackiewicz, MSc, for performing the laboratory tests, necessary to define selected parameters of the system under study and to verify the results of the simulation (Fig.6).

The publication was partly sponsored by the State Committee for Scientific Research under grant No. 9T12C01011.

### References

1. APETAUR M., 1993, Modelling of Transient Non-linear Tyre Responses, *Supplement to Vehicle System Dynamics*, **21**, 116-126
2. BACIŃSKI ST., 1969, Badanie sil i prześlizgów występujących w strefie styku opony terenowej z podłożem nieodkształcalnym, *1-sze Sympozjum Inst. Poj. Mech. i Maszyn Roboczych WAT, Referaty*, 1, Warszawa
3. BAKKER E., NYBORG L., PACEJKA H.B., 1987, Tyre Modelling for Use in Vehicle Dynamics Studies, *SAE Paper* 870421
4. BERKEFELD V., 1983, Der Einfluss der Elastizitäten in Radaufhängung und Lenkung auf das Eigenlenkverhalten von Kraftfahrzeugen, Dissertation, TU München
5. BERNARD J., VANDERPLOEG M., JANE R., 1981, Tire Models for Determination of Vehicle Loads, *Proceedings of 7th IAVSD Symposium*, Cambridge UK
6. BIELECKI Z., 1976, Identyfikacja właściwości dynamicznych pneumatyków pracujących ze zmiennym ciśnieniem powietrza, Rozprawa doktorska, Wydział MEiL Politechniki Warszawskiej
7. BIELECKI Z., MARYNIAK J., 1978, Wyznaczanie doświadczalne charakterystyk dynamicznych kół pneumatycznych pojazdów samochodowych, *Archiwum Budowy Maszyn*, 3
8. BOBROWSKI M., PROCHOWSKI L., 1989, Komputerowa analiza stref poślizgu ogumienia, *Technika Motoryzacyjna*, 6, VII-IX
9. BÖHM F., 1979, Comfort, Vibration and Stress of the Belted Tire, *Proceeding of 6th IAVSD Symposium*, TU Berlin, 30-50
10. BÖHM F., 1989, Models for the Radial Tire for High Frequent Rolling Contact, *Supplement to Vehicle System Dynamics*, **18**, 72-83
11. BÖHM F., 1993, Tire Models for Computational Car Dynamics in the Frequenty Range up to 1000 Hz, *Supplement to Vehicle System Dynamics*, **21**, 82-91
12. CAPTAIN K.M., BOGHANI A.B., WORMLEY D.N., 1979, Analytical Tire Models for Dynamic Vehicle Simulation, *Vehicle System Dynamics*, **8**, 1-32
13. CLARK S.K. (EDIT.), 1981, *Mechanics of Pneumatic Tires*, Washington D.C.
14. CRONIN D.L., 1981, McPherson Strut kinematics, *Mechanism and Machine Theory*, **16**, 6, 631-644
15. DAVIS D.C., 1975, A Radial-Spring Terrain-Enveloping Tire Model, *Vehicle System Dynamics*, **4**, 55-69

16. DUGOFF H., FANCHER P.S., SEGEL L., 1970, An Analysis of Tire Traction Properties and their Influence on Vehicle Dynamic Performance, *SAE Paper* 700377
17. DUNN J.W., OLATUNBOSUN O.A., 1989, Linear and Non-Linear Modelling of Vehicle Rolling Tyre Low Frequency Dynamic Behaviour, *Supplement to Vehicle System Dynamics*, **18**, 179-189
18. FANCHER P.S. JR., BAREKET Z., 1993, Including Roadway and Tread Factors in Semi-Empirical Model of Truck Tyres, *Supplement to Vehicle System Dynamics*, **21**, 92-107
19. FORTUNKOV D.F., 1980, Issledovanie stabilizimiyushchikh momentov upravlyayemykh koles avtomobilya. *Avtomobilnaya promyshlennost*, **10**, 19-21
20. GIM G., NIKRAVESH P.E., 1990, An Analytical Model for Pneumatic Tyres for Vehicle Dynamic Simulation, Part 1: Pure Slips, *International Journal of Vehicle Design*, **11**, 6, 589-618
21. GIM G., NIKRAVESH P.E., 1991, An Analytical Model for Pneumatic Tyres for Vehicle Dynamic Simulation, Part 2: Comprehensive Slips, *International Journal of Vehicle Design*, **12**, 1, 19-39
22. GIM G., NIKRAVESH P.E., 1991, An Analytical Model for Pneumatic Tyres for Vehicle Dynamic Simulation, Part 3: Validation Against Experimental Data, *International Journal of Vehicle Design*, **12**, 2, 217-228
23. GORAJ Z.J., 1982, Selfexcited Vibrations of the Tire, *Vehicle System Dynamics*, **11**, 345-362
24. HILLER M., WOERMIE CH., 1985, Bewegungsanalyse einer Fünfpunkt-Radaufhängung, *ATZ* **87**, 2, 59-64
25. JACKOWSKI J., PROCHOWSKI L., 1994, Analiza sztywności promieniowej ogumienia – metody badań i osiągnane rezultaty, – warunki badań i osiągnane rezultaty, *Biuletyn Wojskowej Akademii Technicznej*, **XLIII**, 1, 25-64
26. JĘDRZEJCZAK A., 1980, Modele współpracy opony z nawierzchnią, *Technika Motoryzacyjna*, **8**, 13-19
27. KAMIŃSKI E., POKORSKI J., 1983, *Teoria samochodu. Dynamika zawieszon i układów napędowych pojazdów samochodowych*, WKiL, Warszawa
28. KHACHATUROV A.A. (EDIT.) ET AL., 1976, *Doroga, shina, avtomobil, voditel*, Mashinostroenie, Moskva
29. KNAPCZYK J., KURANOWSKI A., 1986, Analysis of the Characteristics of the McPherson Suspension Taking Silentblocks Flexibility into Consideration, *Archiwum Budowy Maszyn*, **XXXIII**, 1, 95-105
30. KNAPCZYK J., KURANOWSKI A., 1987, The Analysis of McPherson Suspension and Steering System Flexibility and its Influence on the Wheel Guidance, *Archiwum Budowy Maszyn*, **XXXIV**, 2, 209-223
31. LOMAKO D.M., VEREMEEV N.N., 1993, Modelirovanie sglazivayushchiei sposobnosti pnevmaticheskoi sziny pri issledovanii kolebaniya avtomobilya, *Zeszyty Naukowe Politechniki Świętokrzyskiej, Mechanika*, **49**, Kielce, 259-272
32. LOZIA Z., 1985, Wybrane zagadnienia symulacji cyfrowej procesu hamowania samochodu dwuosowego na nierównej nawierzchni drogi, Rozprawa doktorska, Wyd. SiMR PW, Warszawa

33. LOZIA Z., 1988, A Two-Dimensional Model of the Interaction Between a Pneumatic Tire and an Even and Uneven Road Surface, *Supplement to Vehicle System Dynamics*, **17**, 227-238
34. LOZIA Z., 1993, ZL3DSYM. Program do symulacji ruchu samochodu dwuosioowego. Możliwości i ograniczenia, *Autoprogress'93. Referaty*, Konferencja org. przez PIMot Warszawa, WITPiS Sulejówek, SIMP – Sekcję Samochodową, Jachranka, **III**, 51-62
35. LOZIA Z., STEGIENKA I., 1996, Biaxial Vehicle Motion Simulation and Animation, *Supplement to Vehicle System Dynamics*, **25**, 426-437
36. LUGNER P., 1981, Horizontal Motion of Automobiles. Part I. Theoretical and Practical Investigations. *CISM-Course "Dynamic of High Speed Vehicles"*, Udine, 14-18
37. MAALEJ A.Y., GUENTHER D.A., ELLIS J.R., 1989, Experimental Development of Tyre Force and Moment Models, *International Journal of Vehicle Design*, **10**, 1, 34-51
38. MARYNIAK J., 1976, Dynamiczna teoria obiektów ruchomych, *Prace Naukowe Politechniki Warszawskiej, Mechanika*, **32**
39. MASTINU G., FAINELLO M., 1992, Study of Pneumatic Tyre Behaviour on Dry and Rigid Road by Finite Element Method, *Vehicle System Dynamics*, **21**, 3, 143-165
40. MITSCHKE M., 1977, *Dynamika samochodu*, WKL, Warszawa
41. NORDMARK S., 1984, VTI Driving Simulator. Mathematical Model of a Four-wheeled vehicle for Simulation in Real Time, VTI Report No 267A
42. PACEJKA H.B., 1972, Analysis of Dynamic Response of a Rolling String-Type Tire Model to Lateral Wheel-Plane Vibrations, *Vehicle System Dynamics*, **1**, 37-66
43. PACEJKA H.B., 1981, In-Plane and Out-of-Plane Dynamics of Pneumatic Tires, *Vehicle System Dynamics*, **10**, 221-251
44. PACEJKA H.B., BAKKER E., 1993, The Magic Formula Tyre Model, *Supplement to Vehicle System Dynamics*, **21**, 1-18
45. PACEJKA H.B., SHARP R.S., 1991, Shear Force Development by Pneumatic Tyres in Steady State Conditions: a Review of Modelling Aspects, *Vehicle System Dynamics*, **20**, 3-4, 121-176
46. PALKOVICS L., EL-GINDY M., 1993, Neural Network Representation of Tyre Characteristics: the Neuro-Tyre, *International Journal of Vehicle Design*, **14**, 5/6, 563-591
47. PALKOVICS L., EL-GINDY M., PACEJKA H. B., 1994, Modelling of the Cornering Characteristics of Tyres on an Uneven Road Surface: a Dynamic Version of the "Neuro-Tyre", *International Journal of Vehicle Design*, **15**, 1-2, 189-215
48. PARRAGA G.J., 1971, Steering. A Mathematical Study of the Displacements and Forces Acting in the Steering Elements of a Vehicle, *Automobile Engineer*, 30-36

49. SAKAI H., 1981a, Theoretical and Experimental Studies on the Dynamic Properties of Tyres. Part 1: Review of Theories of Rubber Friction, *International Journal of Vehicle Design*, **2**, 1, 78-110
50. SAKAI H., 1981b, Theoretical and Experimental Studies on the Dynamic Properties of Tyres. Part 2: Experimental Investigation of Rubber Friction and Deformation of Tyre, *International Journal of Vehicle Design*, **2**, 2, 182-226
51. SAKAI H., 1981c, Theoretical and Experimental Studies on the Dynamic Properties of Tyres. Part 3: Calculation of the Six Components of Force and Moment of a Tyree, *International Journal of Vehicle Design*, **2**, 3, 335-372
52. SAKAI H., 1982, Theoretical and Experimental Studies on the Dynamic Properties of Tyres. Part 4: Investigations of the Influences of Running Conditions by Calculation and Experiment, *International Journal of Vehicle Design*, **3**, 3, 333-375
53. SHARP R.S., EL-NASHAR M.A., 1986, A Generally Applicable Digital Computer Based Mathematical Model for Generation of Shear Forces by Pneumatic Tyres, *Vehicle System Dynamics*, **15**, 187-209
54. SHARP R.S., EL-NASHAR M.A., 1993, Tyre Structural Mechanisms Influencing Shear Force Generation: Ideas from a Multi-Radial-Spoke Model, *Supplement to Vehicle System Dynamics*, **21**, 145-155
55. SPRINGER H., ECKER H., SLIBAR A., 1989, A New Analytical Model to Investigate Transient Rolling Conditions of a Steel-Belted Tire, *Supplement to Vehicle System Dynamics*, **17**
56. STUDZIŃSKI K., 1980, *Samochód. Teoria, konstrukcja i obliczanie*, WKiŁ, Warszawa
57. TAKAHASHI T., PACEJKA H.B., 1988, Cornering on Uneven Roads, *Supplement to Vehicle System Dynamics*, **17**
58. WATANABE Y., 1984, A Finite Element Model for Analysis of Deformations of Bias-Ply Motorcycle Tires Subject to Inflation Pressure, *Vehicle System Dynamics*, **13**, 113-128
59. WICHER J., 1995, Wektorowa analiza obciążeń układu kierowniczego samochodu opisanego przestrzennym modelem metematycznym, *Zeszyty Instytutu Pojazdów PW*, **14**, 2, 5-27
60. WILLUMEIT H.P., BÖHM F., 1995, Wheel Vibration and Transient Tire Forces, *Vehicle System Dynamics*, **24**, 525-550
61. ZEGELAAR P.W.A., GONG S., PACEJKA H.B., 1994, Tyre Models for the Study of In-Plane Dynamics, *Supplement to Vehicle System Dynamics*, **23**, 578-590
62. ISO/TC 108/253. Reporting Vertical Road Surface Irregularities. Generalised Vertical Road Inputs to Vehicle

## Model kierowanego koła ogumionego, zagadnienie przestrzenne

### Streszczenie

Artykuł przedstawia model kierowanego koła ogumionego, umożliwiający opis oddziaływania z równą i nierówną nawierzchnią drogi, w stanach ustalonych i nieustalonych. Uwzględniono charakterystyczne dla koła kierowanego, przestrzenne usytuowanie osi sworzni zwrotnicy (osi zataczania) oraz własności sprężyste opony i układu kierowniczego. Model stanowi kompromis między wymaganiami: dokładności opisu zjawisk, ograniczenia formalnej złożoności, długości kodu programu, czasu obliczeń i możliwością eksperymentalnej weryfikacji modelu symulacyjnego ruchu samochodu. Opis modelu uzupełniono przykładowymi wynikami obliczeń symulacyjnych oraz weryfikacji eksperymentalnej. Model ten jest od kilku lat z powodzeniem stosowany w symulacji ruchu pojazdów dwuosiowych.

*Manuscript received August 22, 1996; accepted for print February 12, 1997*